IEEE Access
Multidisciplinary | Rapid Review | Open Access Journal

Received October 5, 2019, accepted October 19, 2019, date of publication October 29, 2019, date of current version November 14, 2019.

Digital Object Identifier 10.1109/ACCESS.2019.2950097

Non Integer Order Modeling and Control of Aerodynamic Load Simulator System

NASIM ULLAH, (Member, IEEE), AND AHMAD AZIZ AL-AHMADI
Electrical Engineering Department, Taif University, Taif 21974, Saudi Arabia
Corresponding author: Nasim Ullah (nasimullah@tu.edu.sa)

ABSTRACT This article investigates the non-integer order model and the controller for aerodynamic load simulator system using fractional order adaptive fuzzy back stepping method. Extra torque disturbance is analyzed using fractional mathematics and a non-integer state predictor is proposed for the estimation of the state vector. For the lumped uncertainty, a fractional order compensation control is formulated using Lyapunov method. Algebraic estimator is derived to estimate the unknown parameters of the system. The proposed controller is simpler in structure and robust to noise, initial conditions. Simulation results authenticate the performance of the proposed control method.

INDEX TERMS Aerodynamic load simulator, fractional order calculus, adaptive fuzzy back stepping control, algebraic parameters estimation, fuzzy logic system, state estimation.

I. INTRODUCTION

Ahigh performance servo actuation system is a crucial part of the guided flight vehicles. Hardware in the loop simulators play an important role in the laboratory based testing and qualification of the aircraft,s actuation system, thus its utilization saves the cost associated with field trials and also reduces human labor. The primary function of the actuation system is to drive the control surfaces of the aircraft. During real flights, the aerodynamic forces and torques are introduced on the control surfaces of the flight vehicle. The applied aerodynamic forces and torques act as load disturbances for the actuation system. To qualify the flight actuators, a load simulator test bench is used in the laboratory environment. Generally a load simulator system consists of a loading motor and the actuator under test. The loading motor is directly coupled to the loaded actuator, so the mathematical dynamics of the hybrid system are very complex. There are three types of load simulator systems that are categorized as hydraulic, pneumatic and electrical types [1].

For the electrical load simulator system (ELS), the details of the integer order modeling and control system are presented in author's previous work [1], [2]. The electro-mechanical systems are associated with several nonlinear factors that need to be addressed using feedback control system. These factors include the nonlinear friction, external disturbances, mechanical vibrations and parametric uncertainties. Beside these phenomenons, the most important factor which has to be considered in the formulation of the control law for ELS is the extra torque disturbance. The extra torque disturbance is induced in the loading motor due the movement of the loaded actuator [3]–[5]. Extra torque disturbance is a function of the velocity, acceleration and the jerk's difference between the loading and loaded motors thus the overall inertia of the system should be exactly known [6]. Practically it is hard to calculate the total inertia of the system, so the control methods presented by the authors of [3]–[7] are not being very effective practically. Although the disturbance due to the velocity component has been compensated but the acceleration and jerk differences have not been considered. To effectively compensate the extra torque disturbance, friction and uncertainties, a robust control law is presented using back stepping method [8]. In [9], a robust compound control method is formulated for the electro-hydraulic load simulator, which is subject to the extra torque disturbance, multi-channel cross coupling and uncertainties. The compound control is robust assuming that the dynamics of the system are exactly known. Since the dynamics of the system are very complex, so practically the control performance may deteriorate since there is no adaptive component formulated for the control law preseted in [9].

Adaptive robust control methods have been proposed in [8]–[13] for electro-hydraulic load simulator systems. A nonlinear integer order mathematical model is developed

The associate editor coordinating the review of this manuscript and approving it for publication was Shihong Ding.

in [1] and adaptive fuzzy back stepping torque control method is proposed for the torque tracking loop of the electrical load simulator system. Control performance of a feedback loop also depends on the identification and compensation of the nonlinear friction. Most of the previous work presented in the literature is focused on the friction compensation using empirical model based approach. The nonlinear friction phenomena associated with electro-hydraulic load simulator system, is compensated using LuGre model [14], adaptive function [15] and modified LuGre model [16]. Model based friction compensation may be ineffective because it indirectly depends on the accuracy of identified parameters. If the model parameters are not estimated accurately then the model based friction compensation may lead to poor control performance. Friction compensation through adaptive algorithms is effective but it is hard to tune the learning rates. Fuzzy and neural networks have been proposed to compensate the nonlinear friction for the robot manipulators [17], [18] but the approximation error may lead to poor performance of the closed loop control system [19]. The unknown or uncertain system parameters have also an adverse effects on the system control performance so it must be estimated online or offline. Algebraic method is a well-known method for the online parameters adaptation which is robust against noise and nonzero initial conditions. Algebraic method is proposed in [1], [20], [21] to estimate the unknown system parameters.

To formulate a model based adaptive robust direct torque control, it is essential to estimate the state vector of the system. In ELS system, an analog torque sensor is used for the measurement of loading torque, but these sensors induce a lot of noise in the feedback signal. Similarly mechanical vibrations may override the electrical signal recorded from the analog torque sensor. So practically it is almost impossible to formulate a model based control law using the measured feedback signal or its derivative. Various techniques have been reported in [23]–[27] for the estimation of state vector in the direct torque control applications. The above cited literature deals with the integer order modeling and control of the load simulator systems. Nowadays fractional calculus is the focus of research community which is widely applied by the automatic control engineers and scientists. The first fractional order controller ''CRONE'' was proposed in 1996 [27]. Later on the researchers extended the application of fractional calculus to other advanced control methods such as sliding mode and terminal sliding mode controllers [29], [30]. Apart from the non-integer controllers, fractional order modeling has emerged as a new topic of interest. In this regard some recent experimental results have been published in [31]. In the published work [31], it has been shown that fractional order controllers based on fractional order system models exhibit additional advantages such as low power and low memory consumption when implemented over the processors. A robust control system based on fractional order model of a permanent magnet synchronous machine is discussed in [32]. The authors have explained the fractional order model identification process in a detailed manner. Similarly the fractional order model and a control system for a robotic manipulator is proposed in [33]. In [34] the authors presented the passive implementation of fractional order impedance using fractional RLC circuits and elements. The solution of a fractional order continuously variable order spring mass damper equation is presented in [35] and the applications of fractional order DC motor model for control system design is discussed in [36]. In the author's previous work, a fractional order fuzzy back stepping controller is proposed [39]. Although it has been shown that the fractional order controllers perform better as compared to the integer order but since the controllers are formulated using integer order dynamics of the ELS system, so the advantages presented in [31] have not been exploited. The hardware realization of fractional order controllers is presented in [40] and [41] and its detailed stability analysis is given in [42].

Based on the above literature survey, this work is focused on deriving a fractional order dynamic model of the ELS system and then using the derived model a non-integer adaptive fuzzy back stepping torque control law is formulated. The proposed fractional order control law is different in formulations as compared to the author's previous work [1]. A non-integer state predictor is proposed for the estimation of the state vector and the algebraic method is used to estimate the unknown parameters of the system. Moreover to estimate the uncertainty, adaptive laws are derived using fractional order Lyapunov function. The proposed control has more degree of freedom as compared to its integer order version presented in [1]. A control component namely transient performance controller [1] is eliminated and it is verified from the numerical simulations that the transient response of the system is enhanced using fractional order tuning. As compared to [1] and from the methodological point of view the original contribution of this proposal is obvious from the following:

1: Mathematical treatment of fractional calculus is totally different from the integer calculus.

2: The previous integer order model of the ELS system [1] has been extended to the fractional order model(Eq. 22-24.)

3: With the fractional order model the derivation of the fractional order control system is different as compared to the integer order controller [1].

4: In the proposed work, the first derivative of the Lyapunov function contains fractional order terms so the mathematical treatment of Eq. 33, 34 and so on is quite different from the previous work [1]

5: In this work, the non-integer model parameters of the actual system are estimated from the experiment while in the previous work this part was not discussed.

7: The derived adaptive laws given in Eq. 41 and the algebraic estimator on Eq. 53 are non-integer.

The rest of the paper is organized as following. In section 2 the readers are introduced with the basics of the fractional calculus, analysis of extra torque disturbance and the non-integer modeling of ELS system. In section 3, the fractional order controller is derived step by step and section 4

discusses the results. Finally the conclusion is made in section 5.

II. FRACTIONAL ORDER MATHEMATICAL MODELING AND ANALYSIS OF EXTRA TORQUE

All the previous research work is focused on the integer order modeling and control of ELS system. But in practice, the dynamics of the physical elements like Inductor and capacitor can be modeled using fractional calculus. To identify the accurate dynamics of the system and for formulation of control law, it is necessary to understand the basics of the fractional calculus.

Definition 1: The Riemann–Liouville fractional order integration and derivative of a function $f(t)$are expressed as shown in Eq. 1 and Eq. 2 [37], [38].

$$ {}_{t_0}I_t^{\alpha} f(t) = D_t^{-\alpha} f(t) = \frac{1}{\Gamma(\alpha)} \int_{t_0}^{t} \frac{f(\tau)}{(t-\tau)^{1-\alpha}} d\tau \tag{1} $$

$$ {}_{t_0}D_t^{\alpha} f(t) = \frac{d^{\alpha}}{dt^{\alpha}} f(t) = \frac{1}{\Gamma(m-\alpha)} \frac{d^m}{dt^m} \int_{t_0}^{t} \frac{f(\tau)}{(t-\tau)^{\alpha-m+1}} d\tau \tag{2} $$

Here $\Gamma(.)$ represents the gamma function,, $m \in N$ and $m-1 < \alpha \leq m$

From Eq. 1 and Eq. 2 the following relation holds: ${}_{t_0}D_t^{\alpha}({}_{t_0}I_t^{\alpha} f(t)) = f(t)$

Definition 2: The Caputo fractional order derivative of a function $f(t)$ is given by [37], [38].

$$ {}_{t_0}D_t^{\alpha} f(t) = \begin{cases} \dfrac{1}{\Gamma(m-\alpha)} \displaystyle\int_{t_0}^{t} \frac{f^{(m)}(\tau)}{(t-\tau)^{\alpha-m+1}} d\tau; & m-1 < \alpha < m \\ \dfrac{d^m}{dt^m} f(t);, & \alpha = m \end{cases} \tag{3} $$

From [37], the Caputo fractional order integral is similarly expressed as of Eq. 1. So by combining Eq. 1 and Eq. 3 the following relation also holds true for Caputo definitions: ${}_{t_0}D_t^{\alpha}({}_{t_0}I_t^{\alpha} f(t)) = f(t)$. Rieman-Liouville and Caputo definitions are very much similar; the only difference lies in dealing with the initial conditions. In Rieman-Liouville definition, the initial conditions are non-integer while for Caputo definition they are of integer order.

Definition 3: Laplace transform of a fractional order derivative of a function is defined as following [41].

$$ \mathcal{L}(D^{\alpha} f) = s^{\alpha} F(s) - \sum_{i=0}^{m-1} s^{\alpha-i-1} f^{(i)}(0) \; ; \; m-1 < \alpha \leq m \tag{4} $$

Here **i** and **m** represent integer numbers. In this work fractional operator is approximated using Oustaloup recursive method [27]. Let the fractional operator be represented as;

$$ W(s) = s^{\alpha} \quad ; \alpha \in R^{+} \; ; \tag{5} $$

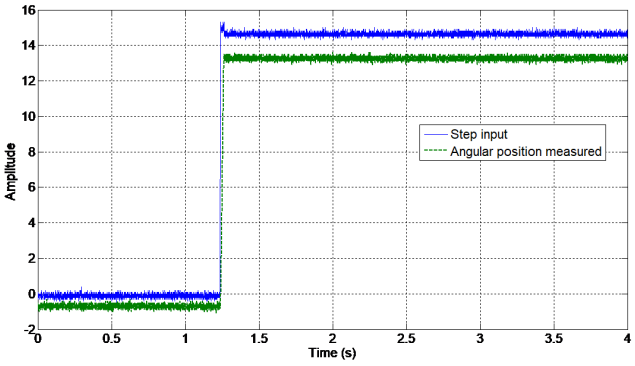

FIGURE 1. Applied step command and motor angular response.

Let the function **W(s)** is approximated using a rational function of the form;

$$ \hat{W}(s) = C_0 \prod_{k=-N}^{N} \frac{s + w_k}{s + w'_k} \tag{6} $$

The above function is approximated for a frequency range of $[w_b \;\; w_h]$ using the following relations:

$$ \{w'_k = w_b \left[\frac{w_h}{w_b}\right]^{\frac{k+N+0.5(1-\alpha)}{2N+1}} ; \; w_k = w_b \left[\frac{w_h}{w_b}\right]^{\frac{k+N+0.5(1+\alpha)}{2N+1}} \tag{7} $$

Here $k = -N : N$, $C_0 = {w_h}^{\alpha}$,α represents fractional order, w_b and w_h represent high and low band frequencies. In this work $[w_b \;\; w_h] = [0.001 \;\; 1000]$rad/sec, the approximation order is $N = 4$ and fractional operator is tested in the range between 0 and 1.

Remark 1: In light of the concepts presented in [37], in the rest of the paper the Riemann–Liouville definitions are used for fractional operator.

A. RESEARCH MOTIVATION AND JUSTIFICATIONS

A fractional order controller is proposed for the ELS system using non-integer model. To identify fractional order mechanical and electrical dynamics of the system, a single experiment is performed using permanent magnet synchronous motor (PMSM) with unknown parameters. A step signal of $v_q = +15$Volts is applied to the drive of motor with inverse park/Clark transformation and it moves by 20 degrees which corresponds to $+13.4$ Volts as per the measurement taken from the position sensor. Fig. 1 shows applied command and motor position response. MATLAB parameter estimation toolbox is used to approximate the unknown parameters of the PMSM motor with integer order and fractional order dynamics. The electrical parameters of the motor are assumed to be the same in d and q reference frames. The step command is treated as input and the measured angular response as output for MATLAB parameter estimation toolbox. Nonlinear least square optimization method is selected with 100 maximum iterations and 400 maximum function (evals). ODE4 (Runge- Kutta) solver is used with fixed step size of the order 0.0004 sec. The cost function is the sum of squared errors (SSE). Fig. 2a compares motor's measured

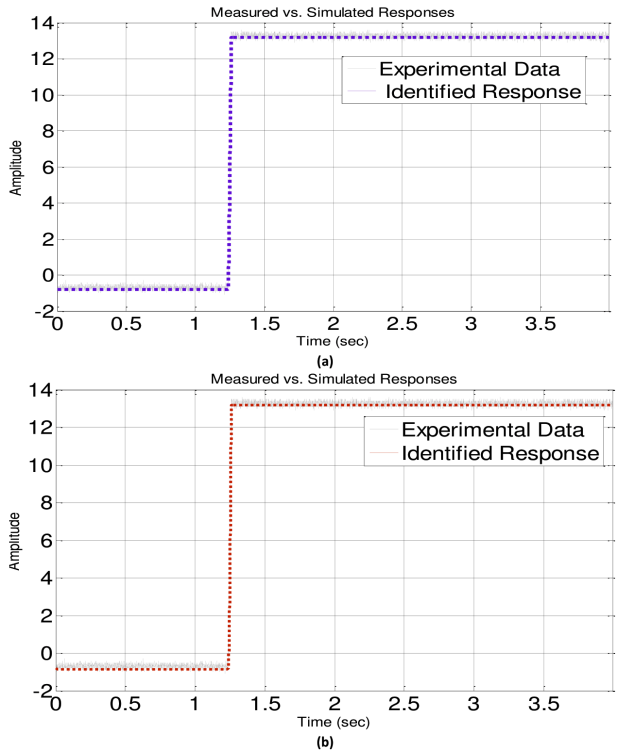

FIGURE 2. Experimental VS identified output response (a) integer order model (b) fractional order model.

TABLE 1. Identified parameters of motor with integer and fractional order dynamics.

Symbol	Integer Order Model	Fractional Order Model
R	$6.2ohms$	$6.2ohms$
L	$4.7mH$	$3.2mH$
J	$0.00045Kg/m^2$	$0.00042Kg/m^2$
B	$.012Nm-s/rad$	$.009Nm-s/rad$
K_t	$15Nm/A$	$14.98Nm/A$
K_b	$0.006Nm/V$	$.008Nm/V$

and identified output response with integer order electrical and mechanical dynamics. The estimated parameters with integer order dynamics are shown in Table. 1. The second case deals with estimation of motor parameters when its electrical and mechanical dynamics are non-integer in nature i.e. $[Ls^{\alpha}+R]^{-1}$ and $[Js^{\alpha}+B]^{-1}$. Here **L** and **R** represent the inductance and resistance of the motor coil; **J** and **B** represent the inertia and damping coefficient and α is the fractional operator. For the second case $\alpha = 0, 8$. Fig. 2b shows system's measured and identified output response with fractional order dynamics. The estimated parameters are given in Table. 1. For the similar identified responses shown in Fig. 2a and Fig. 2b, the estimated parameters for integer and non-integer cases are different. From this experiment it is concluded that the dynamics of the motor can be fractional in nature. It is further concluded that for the nearly same output response the identified system parameters are different. The analysis presented in the above section justifies fractional order representation of the dynamics of the ELS System.

B. FRACTIONAL ORDER MODELING

The assumptions listed in author's previous work [1] are used to derive fractional order model of ELS system.

Assumption 1: System parameters are unknown, slowly time varying and upper bounded such that

$$\begin{aligned} a &= a_n + \Delta a(t) \\ b &= b_n + \Delta b(t) \\ c &= c_n \end{aligned} \tag{8}$$

From [1] we have the following relation;

$$\left\{ b = \frac{K_s K_t}{J R_s}; \quad a = \frac{K_b K_t}{J R_s} + \frac{B}{J}; \; c = \frac{K_s}{J} \right.$$

From (8), $\{a_n\, b_n\, c_n\}$ represent nominal system parameters and $\{a_n\, b_n\, c_n\}$ are assumed to be the slow time varying input gain parameters such that

$$\begin{aligned} a &\in \Omega_1 : \{a_{\min} \le a \le a_{\max}\} \\ b &\in \Omega_2 : \{b_{\min} \le b \le b_{\max}\} \\ c &\in \Omega_3 : \{c_{\min} \le c \le c_{\max}\} \end{aligned} \tag{9}$$

Assumption 2: The unknown system parameters are estimated using algebraic method with finite time convergence property. The effects of slow time varying parameters along with other disturbances have been modeled as lumped disturbance term which is expressed as following:

$$\Psi(t) \in \Omega_4 : f^*(d_{p(t)}, d_{ef}) \tag{10}$$

Here $\Psi(t)$ represents the lumped disturbance and it is represented as $\Psi(t) = c_n d_{ef} + d_{p(t)}$, $f^*(d_{p(t)}, d_{ef})$ is a function of $d_{p(t)}$ and d_{ef}, Ω_4 represents range of disturbance term,$d_{p(t)}$ is disturbance term due to parameters variation and d_{ef} represents fuzzy error. Further details are available in [1].

Assumption 3: To simplify the calculations, electrical dynamics of the system $L_{sq}D^{\alpha}i_q*$ and $L_{sq}D^{\alpha}i_q$ are ignored.

A direct drive permanent magnet synchronous motor (PMSM) acts as ELS system. Sinusoidal back emf of PMSM motor makes it convenient to drive it by sinusoidal excitation waveform with minimum torque ripples [28]. The fractional order dynamics of ELS system in rotating reference frame can be written as

$$\begin{aligned} u_d &= i_d R_s + L_{sd} D^{\alpha} i_d - P L_{sq} i_q w_m \\ u_q &= i_q R_s + L_{sq} D^{\alpha} i_q + P L_{sd} i_d w_m + P \Psi_m w_m \\ T_e &= \frac{3P}{2}[\Psi_m i_q + (L_{sd} - L_{sq}) i_d i_q] = J D^{\alpha} w_m \\ &\quad + B w_m + T_f + T_L \end{aligned} \tag{11}$$

Here D^{α} represents fractional derivative, α is the order of fractional operator. All other parameters of Eq. (11) are given in Appendix B. The simplified model of torque sensor is expressed in Eq. 12.

$$T_L = K_s(\theta_m - \theta_a) \tag{12}$$

To decouple the speed and current dynamics of the system and to achieve largest torque operation, d –axis reference current

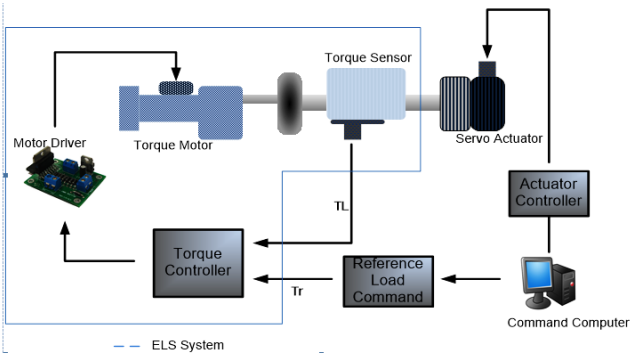

FIGURE 3. ELS system configuration.

i_{dr} is set to zero. The inner loop PI controllers are used to regulate d and q–axis currents. Fig. 3 shows working diagram of ELS system. The following procedures are adopted to derive a meaningful state model

Step1: From Fig. 3 if the servo actuator is following a reference command i.e. $\theta_a \neq 0$ with zero excitation of ELS loading motor, i.e. $u_q = 0$, then as a result of the actuator,s movement, ELS loading motor also moves with following fractional order dynamics;

$$-K_b w_a = i_q*(R_s) + L_{sq} D^{\alpha} i_q* \tag{13}$$

$$T_{sft} - T_e* = -JD^{\alpha} w_a - Bw_a \tag{14}$$

In Eq. (13) $K_b = P\Psi_m$ is the back emf constant.

Step2: If both motors are excited i.e.$\theta_a \neq 0$ and $u_q \neq 0$, then from (11), the fractional order model can be derived as;

$$u_q = (i_q - i_q*)R_s + L_{sq} D^{\alpha}(i_q - i_q*) + K_b(w_m - w_a) \tag{15}$$

$$\begin{aligned} T_e - T_e* &= K_t[i_q - i_q*] = [\frac{3P}{2}\Psi_m][i_q - i_q*] \\ &= JD^{\alpha}(w_m - w_a) + B(w_m - w_a) - T_{sft} + T_f + T_L \end{aligned} \tag{16}$$

As per Assumption 3, by simplifying Eq. (15)one obtains the following expression:

$$(i_q - i_q*) = \frac{u_q - K_b(w_m - w_a)}{R_s} \tag{17}$$

Set $K_t = \frac{3P}{2}\Psi_m$ and by replacing Eq. (17) in Eq. (16), one obtains:

$$\begin{aligned} K_t[\frac{u_q - K_b(w_m - w_a)}{R_s}] = JD^{\alpha}(w_m - w_a) + B(w_m - w_a) \\ - T_{sft} + T_f + T_L \end{aligned} \tag{18}$$

Multiply Eq. (18) by K_s

$$\begin{aligned} &K_s D^{\alpha}(w_m - w_a) \\ &= -K_s[\frac{B}{J} + \frac{K_b K_t}{JR_s}](w_m - w_a) \\ &\quad + (\frac{K_s K_t}{JR_s})u_q - \frac{K_s}{J}(T_{sft} + T_f) - \frac{K_s}{J}T_L \end{aligned} \tag{19}$$

Let $a = [\frac{B}{J} + \frac{K_b K_t}{JR_s}]$, $b = [\frac{K_s K_t}{JR_s}]$, $c = \frac{K_s}{J}$. Similarly Using Eq. (12), $D^{\alpha}\dot{T}_L = K_s D^{\alpha}(w_m - w_a)$ and $\dot{T}_L = K_s(w_m - w_a)$, Eq. (19) is written as

$$D^{\alpha}\dot{T}_L = -a\dot{T}_L + bu_q - cf(T_{extra}, T_f) - cT_L \tag{20}$$

In Eq. (20),the term $cf(T_{extra}$: is expressed as: $cf(T_{extra}, T_f) = \frac{K_s}{J}(T_{sft} + T_f)$. Here $f(T_{extra}, T_f)$ corresponds to the disturbance torque acting on the loading motor due to the actuator's movement and friction. Using assumption 1, Eq. (20) is expressed as following:

$$\begin{aligned} D^{\alpha}\dot{T}_L = -(a_n + \Delta a(t))\dot{T}_L + (b_n + \Delta b(t))u_q \\ - c_n f(T_{extra}, T_f) - c_n T_L \end{aligned} \tag{21}$$

Eq. (21) is simplified as following:

$$\begin{aligned} D^{\alpha}\dot{T}_L &= -a_n\dot{T}_L + b_n u_q \\ &\quad - c_n T_L - c_n f(T_{extra}, T_f) - d_{p(t)} \end{aligned} \tag{22}$$

$$d_{p(t)} = \Delta a(t)\dot{T}_L + \Delta b(t)u_q \tag{23}$$

The lumped disturbance is expressed as $\Psi(t) = c_n d_{ef} + d_{p(t)}$. It consists of fuzzy approximation error and time varying parameters disturbance. A fractional order state predictor is formulated as following:

$$D^{\alpha}\hat{\dot{T}}_L = -a_n\hat{\dot{T}}_L + b_n u_q - c_n\hat{T}_L - c_n\hat{f}(T_{extra}, T_f) + \hat{\Psi}(t) + \Gamma E \tag{24}$$

Here$\hat{f}(T_{extra}, T_f)$ is nonlinear term to be estimated online using fuzzy system, Γ is gain matrix, E represents error between actual plant and state predictor, i.e. $E = e = \hat{T}_L - T_L; \dot{e} = \hat{\dot{T}}_L - \dot{T}_L$. $[\hat{\dot{T}}_L, \hat{T}_L]$ represents state vector to be estimated and $\hat{\Psi}(t)$ is the adaptive controller for the compensation of the lumped disturbances to be derived later on.

III. CONTROL LAW FORMULATION

In this section a fractional order torque control law is derived based on the identified fractional order model presented in Eq. (22). Extra torque and nonlinear friction are compensated using fractional order adaptive fuzzy system. Fractional order algebraic method is used to estimate the unknown parameters of the system. Moreover fractional order lumped uncertainty controller is formulated using Lyapunov method. The working diagram of the overall control system is shown in Fig. 4.

With desired and output loading torque vector $\{T_r\ T_L\}$, the error vector is expressed as following:

$$\{e_1 = T_L - T_r\ ;\ \dot{e}_1 = \dot{T}_L - \dot{T}_r; e_2 = \dot{e}_1 \tag{25}$$

From Fig.4, error dynamics between system and state predictor are formulated as following:

$$e = \hat{T}_L - T_L; \dot{e} = \hat{\dot{T}}_L - \dot{T}_L \tag{26}$$

Using Eq. 22, 24 and 26, the fractional order error dynamics between the actual plant and the state predictor are expressed as Eq. 27.

$$D^{\alpha}\dot{e} = D^{\alpha}\hat{\dot{T}}_L - D^{\alpha}\dot{T}_L = -a_n\dot{e} - c_n e + (\hat{\Psi(t)} - \Psi(t)) + \Gamma E \tag{27}$$

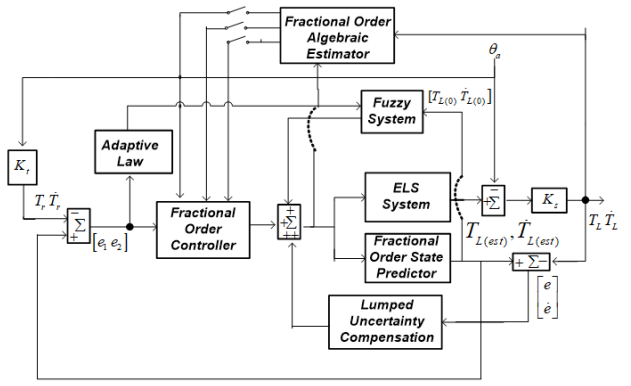

FIGURE 4. Controller working diagram.

In Eq. 27, the lumped uncertainty term is expressed as $\Psi(t) = c_n d_{ef} + d_{p(t)}$, while the factor d_{ef} is written as: $d_{ef} = \hat{f}(T_{extra}, T_f) - f(T_{extra}, T_f)$. From Eq. (25), define the first virtual control law as a function of error in form of Eq. 28.

$$\dot{e}_1 = \alpha_1 - \dot{T}_r \tag{28}$$

Here α_1 represents the first virtual control. Choose a Lyapunov function as $V_1 = \frac{1}{2}{e_1}^2$. From the first derivative of V_1, the first virtual control law is derived as $\alpha_1 = -q_1 e_1 + \dot{T}_r$. By combining α_1 and$\dot{V}_1$ one obtains;

$$\dot{V}_1 = -q_1 {e_1}^2 \tag{29}$$

In Eq. 29 q_1 represents a constant. By letting $q_1 > 0$ the expression in Eq. 29 is rewritten as $\dot{V}_1 < 0$. The second tracking error vector is written as following:

$$[e_2 = \dot{T}_L - \alpha_1 \,; D^\alpha e_2 = D^\alpha \dot{T}_L - D^\alpha \alpha_1] \tag{30}$$

By combining Eq. (22) and Eq. (30), one obtains.

$$D^\alpha e_2 = -a_n \dot{T}_L + b_n u_q - c_n T_L - c_n f(T_{extra}, T_f) - d_{P(t)} - D^\alpha \alpha_1 \tag{31}$$

Using property of fractional order derivatives;$\dot{e}_2 = D^{1-\alpha}(D^\alpha e_2)$ and $\ddot{e} = D^{1-\alpha}(D^\alpha \dot{e})$, choose the second Lyapunov function as expressed in Eq. 32.

$$V_2 = V_1 + \frac{1}{2}{e_2}^2 + \frac{1}{2\eta_i}\sum_{i=1}^{n} D^{-\alpha}\tilde{\theta}_i D^{-\alpha}\tilde{\theta}_i + \frac{1}{2\gamma} D^{-\alpha}(\hat{\Psi}(t) - \Psi(t)) D^{-\alpha}(\hat{\Psi}(t) - \Psi(t)) + \frac{1}{2}\dot{e}^2 \tag{32}$$

In Eq. 32, $\tilde{\theta}_i$ represents an unknown parameter to be estimated by the fuzzy system. Here $\tilde{\theta}_i$ is explicitly utilized to estimate the unknown function $f(T_{extra}, T_f)$. By taking first derivative of Eq. (32)yields:

$$\dot{V}_2 = \dot{V}_1 + e_2 \dot{e}_2 + \frac{1}{\eta_i}\sum_{i=1}^{n} D^{1-\alpha}\tilde{\theta}_i D^{-\alpha}\tilde{\theta}_i + \frac{1}{\gamma} D^{1-\alpha}(\hat{\Psi}(t) - \Psi(t)) D^{-\alpha}(\hat{\Psi}(t) - \Psi(t)) + \dot{e}\ddot{e} \tag{33}$$

$$\dot{V}_2 = \dot{V}_1 + e_2 D^{1-\alpha}[D^\alpha e_2] + \frac{1}{\eta_i}\sum_{i=1}^{n} D^{1-\alpha}\tilde{\theta}_i D^{-\alpha}\tilde{\theta}_i + \frac{1}{\gamma} D^{1-\alpha}(\hat{\Psi}(t) - \Psi(t)) D^{-\alpha}(\hat{\Psi}(t) - \Psi(t)) + \dot{e} D^{1-\alpha}(D^\alpha \dot{e}) \tag{34}$$

Here learning rates of adaptive control system are represented as η_i,γ. By combine Eq. 27, Eq. 31 and Eq. 34, one obtains the following expression.

$$\begin{aligned}\dot{V}_2 = \dot{V}_1 &+ e_2 D^{1-\alpha}[-a_n \dot{T}_L + b_n u_q - c_n T_L - c_n f(T_{extra}, T_f) - d_{p(t)} - D^\alpha \alpha_1] \\ &+ \frac{1}{\eta_i}\sum_{i=1}^{n} D^{1-\alpha}\tilde{\theta}_i D^{-\alpha}\tilde{\theta}_i + \frac{1}{\gamma} D^{1-\alpha}(\hat{\Psi}(t) - \Psi(t)) \\ &* D^{-\alpha}(\hat{\Psi}(t) - \Psi(t)) \\ &+ \dot{e} D^{1-\alpha}(-a_n \dot{e} - c_n e + \hat{\Psi}(t) - \Psi(t) + \Gamma E)\end{aligned} \tag{35}$$

Choose the proposed control law as following:

$$u_q = \frac{1}{b_n}(-q_2 D^{\alpha-1} e_2 + a_n \dot{T}_L + c_n T_L + c_n \hat{f}(T_{extra}, T_f) + D^\alpha \alpha_1) - \frac{1}{b_n} D^{\alpha-1}[k_1 e_2 + k_2 . sgn(e_2)] + \frac{\hat{\Psi}(t)}{b_n} \tag{36}$$

In Eq. (36) k_1 and k_2 represent reaching law gain matrix and q_2 is a constant.

A. STABILITY PROOF

To prove the stability of the closed loop system, combine Eq. (35) and Eq. (36) and the following expression is obtained.

$$\begin{aligned}\dot{V}_2 = &-q_1 e_1^2 - q_2 e_2^2 + e_2 D^{1-\alpha}[c_n \hat{f}(T_{extra}, T_f) - c_n f(T_{extra}, T_f) - d_{p(t)} + \hat{\Psi}(t) - k_1 D^{\alpha-1} e_2 \\ &- k_2 . D^{\alpha-1} sgn(e_2)] + \frac{1}{\eta_i}\sum_{i=1}^{n} D^{1-\alpha}\tilde{\theta}_i D^{-\alpha}\tilde{\theta}_i \\ &+ \frac{1}{\gamma} D^{1-\alpha}(\hat{\Psi}(t) - \Psi(t)) D^{-\alpha}(\hat{\Psi}(t) - \Psi(t)) \\ &+ \dot{e} D^{1-\alpha}(-a_n \dot{e} - c_n e + \hat{\Psi}(t) - \Psi(t) + \Gamma E)\end{aligned} \tag{37}$$

Define fuzzy error d_{ef} as following [17].

$$d_{ef} = f(T_{extra}, T_f) - \tilde{f}(T_{extra}, T_f)^{/\theta *},$$
$$\sum_{i=1}^{n} \tilde{\theta}_i \xi_i(\dot{\theta}_i) = c_n \hat{f}(T_{extra}, T_f)^{/\theta} - c_n \tilde{f}(T_{extra}, T_f)^{/\theta *} \tag{38}$$

By adding and subtracting $c_n \tilde{f}(T_{extra}, T_f)^{/\theta *}$ in Eq. (37), one obtains:

$$\begin{aligned}\dot{V}_2 = &-q_1 e_1^2 - q_2 e_2^2 + e_2 D^{1-\alpha}[\sum_{i=1}^{n} \tilde{\theta}_i \xi_i(\dot{\theta}_i) + (-c_n d_{ef} - d_{p(t)}) \\ &+ \hat{\Psi}(t) - k_1 D^{\alpha-1} e_2 - k_2 . D^{\alpha-1} sgn(e_2)] \\ &+ \frac{1}{\eta_i}\sum_{i=1}^{n} D^{1-\alpha}\tilde{\theta}_i D^{-\alpha}\tilde{\theta}_i\end{aligned}$$

$$+\frac{1}{\gamma}D^{1-\alpha}(\hat{\Psi}(t)\ -\Psi(t))D^{-\alpha}(\hat{\Psi}(t)\ -\Psi(t))$$
$$+\dot{e}D^{1-\alpha}(\hat{\Psi}(t)\ -\Psi(t))+\dot{e}D^{1-\alpha}(-a_n\dot{e}-c_ne+\Gamma E) \quad (39)$$

In Eq. (39),$-\Psi(t)\ =-c_nd_{ef}-d_{p(t)}$. By re- arranging similar terms in Eq. 39, one obtains

$$\dot{V}_2=-q_1e_1^2-q_2e_2^2+[e_2\sum_{i=1}^{n}D^{1-\alpha}\tilde{\theta}_i\xi_i(\dot{\theta}_i)$$
$$+\frac{1}{\eta_i}\sum_{i=1}^{n}D^{1-\alpha}\tilde{\theta}_iD^{-\alpha}\tilde{\theta}_i]+e_2D^{1-\alpha}(\hat{\Psi}(t)\ -\Psi(t))$$
$$+\frac{1}{\gamma}D^{1-\alpha}(\hat{\Psi}(t)\ -\Psi(t))D^{-\alpha}(\hat{\Psi}(t)\ -\Psi(t))$$
$$+\dot{e}D^{1-\alpha}(\hat{\Psi}(t)\ -\Psi(t))-k_1{e_2}^2-k_2.|e_2|$$
$$+\dot{e}D^{1-\alpha}(-a_n\dot{e}-c_ne+\Gamma E) \quad (40)$$

By defining $\tilde{E}_{\Psi(t)}=(\hat{\Psi}(t)\ -\Psi(t))$ the following adaptive laws are derived using Eq. (40)

$$\begin{cases}D^{-\alpha}\tilde{\theta}_i=-\eta_ie_2\xi_i(\dot{\theta}_i)\\ D^{-\alpha}\tilde{E}_{\Psi(t)}=-\gamma^{-1}(e_2+\dot{e})\end{cases} \quad (41)$$

After solving Eq. (40) and Eq. (41) one obtains:

$$\dot{V}_2=-q_1e_1^2-q_2e_2^2+\sum_{i=1}^{n}D^{1-\alpha}\tilde{\theta}_i[e_2\xi_i(\dot{\theta}_i)-e_2\xi_i(\dot{\theta}_i)]$$
$$+D^{1-\alpha}\tilde{E}_{\Psi(t)}[e_2+\dot{e}-e_2-\dot{e}]-k_1{e_2}^2-k_2.|e_2|$$
$$+\dot{e}D^{1-\alpha}(-a_n\dot{e}-c_ne+\Gamma E) \quad (42)$$
$$\dot{V}_2=-q_1e_1^2-q_2e_2^2-k_1{e_2}^2-k_2.|e_2|$$
$$+\dot{e}D^{1-\alpha}(-a_n\dot{e}-c_ne+\Gamma E) \quad (43)$$

From Eq. (43), by letting the term $\dot{e}D^{1-\alpha}(-a_n\dot{e}-c_ne+\Gamma E)=\mu$, Eq. 43 is expressed in the following form:

$$\dot{V}_2=-\varepsilon-k_2.|e_2|+\mu \quad (44)$$

The accumulated term $\varepsilon=-q_1e_1^2-q_2e_2^2-k_1{e_2}^2$ is always negative. From Eq. (44) by choosing $q_1>0, q_2>0, k_1>0, k_2>\mu$,where k_2 is positive, then it is easy to show that the first derivative of the Lyapunov function $\dot{V}_2<0$, so sliding condition exists and $e_2=0$ is zero. From Eq. (29)$\dot{V}_1<0$, it means that $e_1=0; t\to\infty$. When sliding condition occurs, then from Eq. 25 it is concluded that $T_L\approx T_r$ and $\dot{T}_L\approx\dot{T}_r$ which shows that the closed loop system is stable.

B. ALGEBRAIC PARAMETERS ESTIMATION

With perfect compensation control, the simplified version of Eq. (22) is expressed in the following form:

$$D^{\alpha}\dot{T}_L+a_n\dot{T}_L+c_nT_L=b_nu_q$$
$$D^{1+\alpha}T_L+a_n\dot{T}_L+c_nT_L=b_nu_q \quad (45)$$

The algorithm is derived based on the concepts presented in [19], [20]. Using Definition 4, the Laplace transform of

TABLE 2. ELS motor and controller parameters.

ELS Parameter	Value	ELS Parameter	Value
J	0.04 Kg/m^2	q_1/b	.0023
R_s	7.5 ohms	q_2/b	.0047
K_t	5.732 Nm/A	η_i	0.0001
K_b	5.732 Nm/A	γ	2.5
B	0.244 Nm/rad/sec	k_1	1.5
K_s	950 Nm/rad	k_2	0.5
T_sT_c	3 Nm, 2.7 Nm	σ_1	2.5
σ_0	200 Nm/rad	σ_2	.02
$\Gamma_1\Gamma_2$	1.5 2.3		

Eq. (45) yields:

$$\begin{pmatrix}s^{1+\alpha}T_L(s)-s^{\alpha}T_L(0))+a_n(sT_L(s)-T_L(0))\\ +c_nT_L(s)=b_nu_q(s)\end{pmatrix} \quad (46)$$

Multiply (46) by s^2

$$\left(s^{3+\alpha}T_L(s)-s^{2+\alpha}T_L(0)-s^2\dot{T}_L(0)\right)+a_n(s^3T_L(s)$$
$$-s^2T_L(0))+s^2c_nT_L(s)=s^2b_nu_q(s) \quad (47)$$

Take 3rd derivative of (47) with respect to s

$$\frac{d^3}{ds^3}(s^{3+\alpha}T_L(s))+a_n\frac{d^3}{ds^3}(s^3T_L(s))$$
$$+c_n\frac{d^3}{ds^3}s^2T_L(s)=b_n\frac{d^3}{ds^3}(s^2u_q(s)) \quad (48)$$

By expanding Eq. (48), the resultant expression can be written in the following form:

$$\begin{pmatrix}s^{3+\alpha}\frac{d^3}{ds^3}T_L(s)+3(3+\alpha)s^{2+\alpha}\frac{d^2}{ds^2}T_L(s)\\ +3(3+\alpha)(2+\alpha)s^{1+\alpha}\frac{d}{ds}T_L(s)\\ +(3+\alpha)(2+\alpha)(1+\alpha)s^{\alpha}T_L(s)\end{pmatrix}$$
$$+a_n(s^3\frac{d^3}{ds^3}T_L(s)+9s^2\frac{d^2}{ds^2}T_L(s)+18s\frac{d}{ds}T_L(s)$$
$$+6T_L(s))+c_n(s^2\frac{d^3}{ds^3}T_L(s)+6s\frac{d^2}{ds^2}T_L(s)+6\frac{d}{ds}T_L(s))$$
$$=b_n(s^2\frac{d^3}{ds^3}u_q(s)+6s\frac{d^2}{ds^2}u_q(s)+6\frac{d}{ds}u_q(s)) \quad (49)$$

In Eq.(49), the highest derivative of the complex variable is of $3+\alpha^{th}$ order. Multiply Eq. (49) by $s^{-3-\alpha}$

$$\begin{pmatrix}\frac{d^3}{ds^3}T_L(s)+3(3+\alpha)s^{-1}\frac{d^2}{ds^2}T_L(s)+3(3+\alpha)(2+\alpha)\\ *s^{-2}\frac{d}{ds}T_L(s)+(3+\alpha)(2+\alpha)(1+\alpha)s^{-3}T_L(s)\end{pmatrix}$$
$$+a_n(s^{-\alpha}\frac{d^3}{ds^3}T_L(s)+9s^{-\alpha-1}\frac{d^2}{ds^2}T_L(s)+18s^{-\alpha-2}\frac{d}{ds}T_L(s)$$
$$+6s^{-\alpha-3}T_L(s))+c_n(s^{-\alpha-1}\frac{d^3}{ds^3}T_L(s)+6s^{-\alpha-2}\frac{d^2}{ds^2}T_L(s)$$
$$+6s^{-\alpha-3}\frac{d}{ds}T_L(s))=b_n(s^{-\alpha-1}\frac{d^3}{ds^3}u_q(s)+6s^{-\alpha-2}\frac{d^2}{ds^2}u_q(s)$$
$$+6s^{-\alpha-3}\frac{d}{ds}u_q(s)) \quad (50)$$

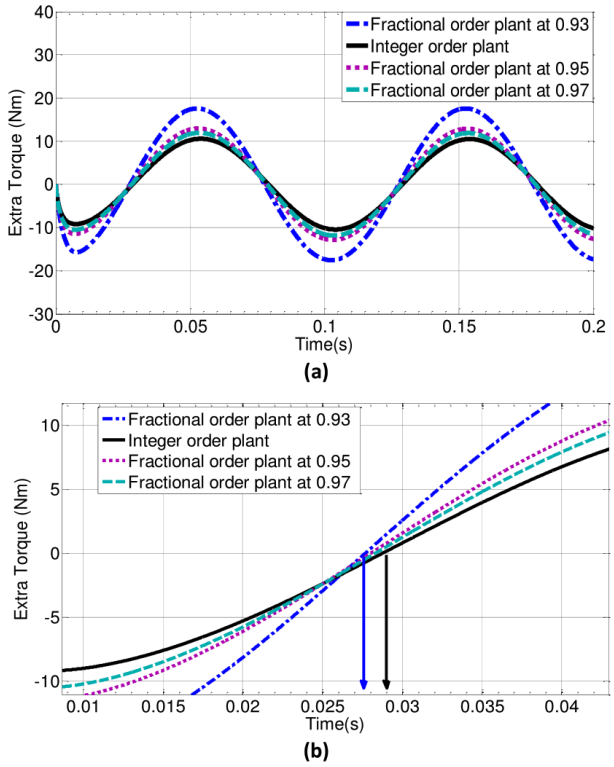

FIGURE 5. a) Extra torque disturbance (b) Enlarged view.

Multiply Eq. (50) by s^{-1} and s^{-2} to get another two equations of the form:

$$\begin{aligned}
&\left(\begin{array}{l} s^{-1}\dfrac{d^3}{ds^3}T_L(s) + 3(3+\alpha)s^{-2}\dfrac{d^2}{ds^2}T_L(s) \\ +3(3+\alpha)(2+\alpha)s^{-3}\dfrac{d}{ds}T_L(s) + (3+\alpha) \\ *(2+\alpha)(1+\alpha)s^{-4}T_L(s) \end{array}\right) \\
&+ a_n(s^{-\alpha-1}\frac{d^3}{ds^3}T_L(s) + 9s^{-\alpha-2}\frac{d^2}{ds^2}T_L(s) \\
&+ 18s^{-\alpha-3}\frac{d}{ds}T_L(s) + 6s^{-\alpha-4}T_L(s)) + c_n(s^{-\alpha-2}\frac{d^3}{ds^3}T_L(s) \\
&+ 6s^{-\alpha-3}\frac{d^2}{ds^2}T_L(s) + 6s^{-\alpha-4}\frac{d}{ds}T_L(s)) = b_n(s^{-\alpha-2}\frac{d^3}{ds^3}u_q(s) \\
&+ 6s^{-\alpha-3}\frac{d^2}{ds^2}u_q(s) + 6s^{-\alpha-4}\frac{d}{ds}u_q(s)) \qquad (51)
\end{aligned}$$

$$\begin{aligned}
&\left(\begin{array}{l} s^{-2}\dfrac{d^3}{ds^3}T_L(s) + 3(3+\alpha)s^{-3}\dfrac{d^2}{ds^2}T_L(s) \\ +3(3+\alpha)(2+\alpha)s^{-4}\dfrac{d}{ds}T_L(s) \\ +(3+\alpha)(2+\alpha)(1+\alpha)s^{-5}T_L(s) \end{array}\right) \\
&+ a_n(s^{-\alpha-2}\frac{d^3}{ds^3}T_L(s) + 9s^{-\alpha-3}\frac{d^2}{ds^2}T_L(s) \\
&+ 18s^{-\alpha-4}\frac{d}{ds}T_L(s) + 6s^{-\alpha-5}T_L(s)) + c_n(s^{-\alpha-3}\frac{d^3}{ds^3}T_L(s) \\
&+ 6s^{-\alpha-4}\frac{d^2}{ds^2}T_L(s) + 6s^{-\alpha-5}\frac{d}{ds}T_L(s)) = b_n(s^{-\alpha-3}\frac{d^3}{ds^3}u_q(s) \\
&+ 6s^{-\alpha-4}\frac{d^2}{ds^2}u_q(s) + 6s^{-\alpha-5}\frac{d}{ds}u_q(s)) \qquad (52)
\end{aligned}$$

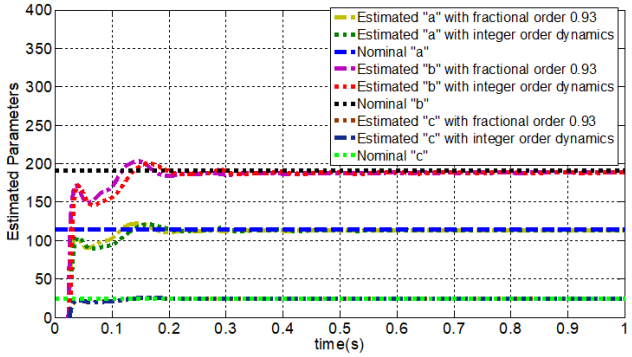

FIGURE 6. Estimated parameters.

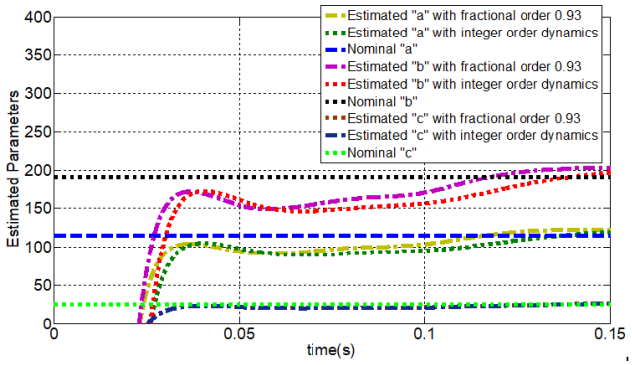

FIGURE 7. Enlarged view.

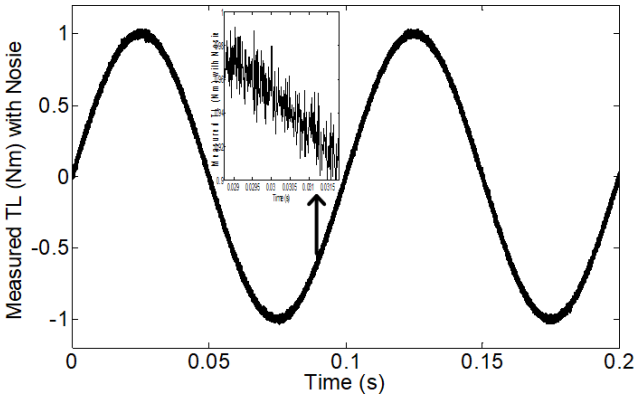

FIGURE 8. Measured T_L with noise.

Re arranging Eq. (50), (51) and (52)

$$\begin{aligned}
a_nA_{11} + b_nA_{12} + c_nA_{13} &= B_1 \\
a_nA_{21} + b_nA_{22} + c_nA_{23} &= B_2 \\
a_nA_{31} + b_nA_{32} + c_nA_{33} &= B_3 \qquad (53)
\end{aligned}$$

Expression (53) can be represented in matrix form as following:

$$\begin{bmatrix} A_{11} & A_{12} & A_{13} \\ A_{21} & A_{22} & A_{23} \\ A_{31} & A_{32} & A_{33} \end{bmatrix} \begin{bmatrix} a_n \\ b_n \\ c_n \end{bmatrix} = \begin{bmatrix} B_1 \\ B_2 \\ B_3 \end{bmatrix} \qquad (54)$$

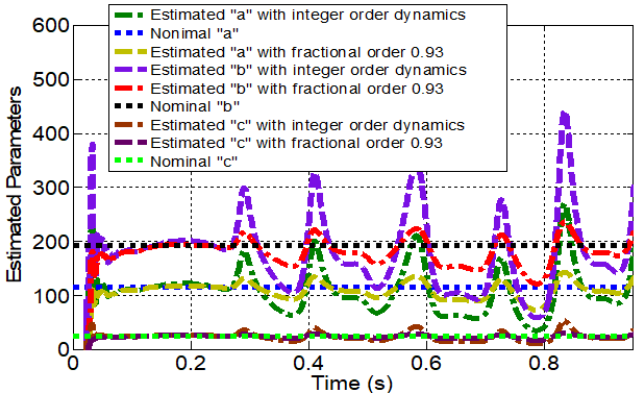

FIGURE 9. Estimated parameters from noise measurement.

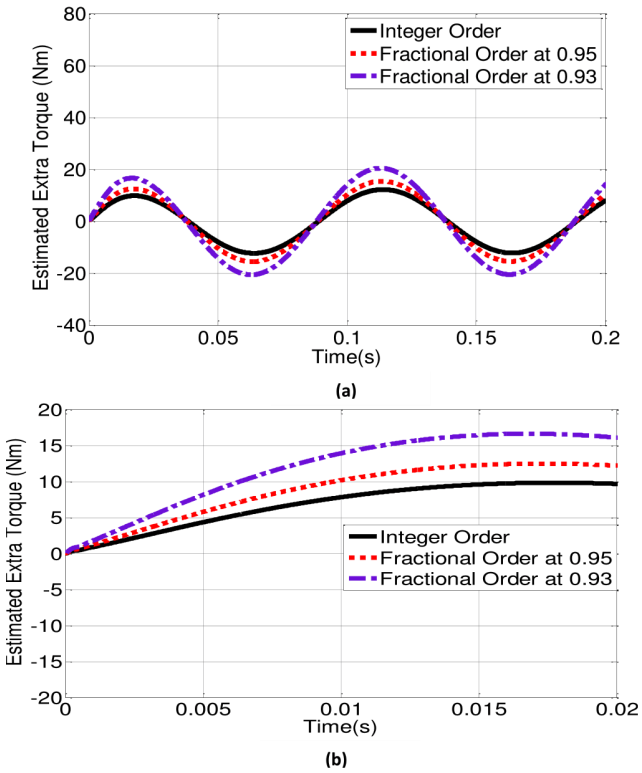

FIGURE 10. (a) Estimation of extra torque (b) Enlarged view.

From theory of linear algebra the solution is written in the form given below.

$$a_n = \frac{\begin{vmatrix} B_1 & A_{12} & A_{13} \\ B_2 & A_{22} & A_{23} \\ B_3 & A_{32} & A_{33} \end{vmatrix}}{\begin{vmatrix} A_{11} & A_{12} & A_{13} \\ A_{21} & A_{22} & A_{23} \\ A_{31} & A_{32} & A_{33} \end{vmatrix}}, \quad b_n = \frac{\begin{vmatrix} A_{11} & B_1 & A_{13} \\ A_{21} & B_2 & A_{23} \\ A_{31} & B_3 & A_{33} \end{vmatrix}}{\begin{vmatrix} A_{11} & A_{12} & A_{13} \\ A_{21} & A_{22} & A_{23} \\ A_{31} & A_{32} & A_{33} \end{vmatrix}},$$

$$c_n = \frac{\begin{vmatrix} A_{11} & A_{12} & B_1 \\ A_{21} & A_{22} & B_2 \\ A_{31} & A_{32} & B_3 \end{vmatrix}}{\begin{vmatrix} A_{11} & A_{12} & A_{13} \\ A_{21} & A_{22} & A_{23} \\ A_{31} & A_{32} & A_{33} \end{vmatrix}} \tag{55}$$

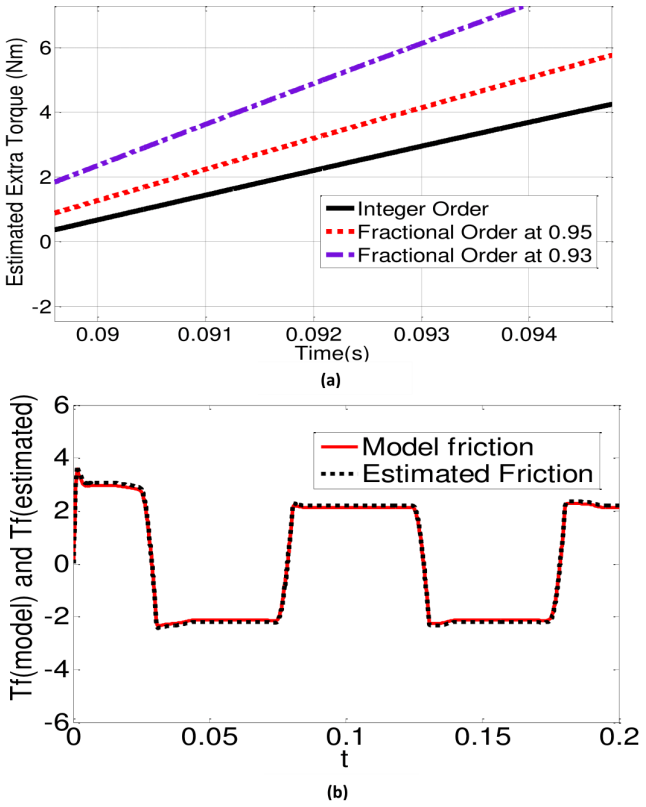

FIGURE 11. (a) Phase response of estimated extra torque (b) Estimated friction torque.

In Eq. (54) the coefficients of 3x3 matrix are recorded in Appendix (A).

IV. RESULTS AND DISCUSSION

Simulink tool of *MATLAB* software is used for validating the promising performance of the proposed control scheme.To verify the effectiveness of proposed method, the parameters of ELS system and controller are given in Table 2.

A. EXTRA TORQUE ANALYSIS AND SIMULATION

Extra torque acts on loading motor due to the movement of the loaded actuator. The input command of loading motor is set to zero. It means that $u_q = 0$. Reference command of loaded actuator is set to 10 degrees. Fig. 5a and 5b show the induced extra torque in the loading motor with both the integer order and fractional order dynamic model. From Fig. 5a, 10 Nm peak to peak extra torque disturbance is induced with integer order model.The disturbance torque peak increases further as we use and decrease the fractional order of the non-integer model. The peak extra torque is generated when the fractional order of the non- integer model is 0.93. Apart from the magnitude, phases of the induced extra torque with different fractional orders are analyzed in Fig. 5b. At fractional order of 0.93, system dynamics are much faster as compared to integer order model. Moreover the magnitude of the induced extra torque is maximum but at the same time system the dynamics

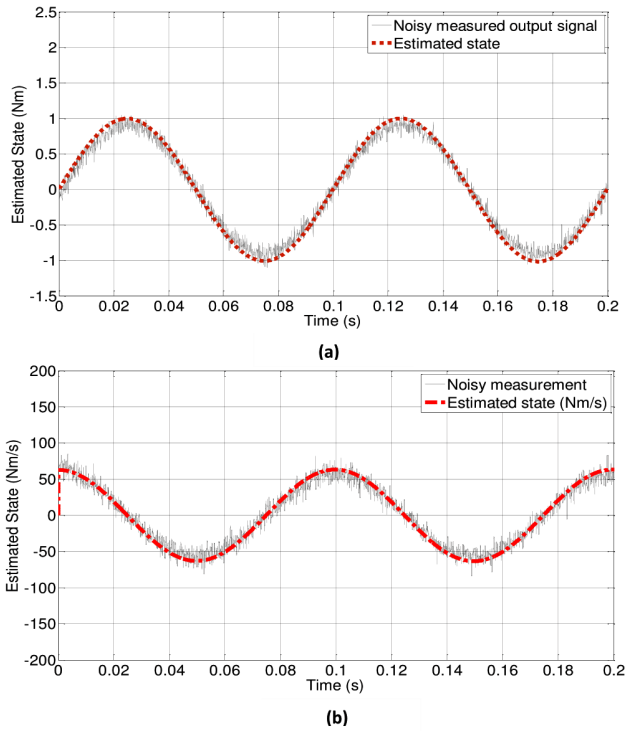

FIGURE 12. (a) estimated torque (Nm) (b) estimated torque derivative (Nm/s).

are faster. With faster dynamics, response of compensation control will be faster which is advantageous.

B. PARAMETERS ESTIMATION COMPARISON

Unknown system parameters are estimated using integer and fractional order algebraic estimation algorithm. After its convergence to true values, both the controller and the state predictor are updated. The estimated system parameters are shown in Fig. 6. The convergence time of the fractional order method is faster as compared to integer order method. Enlarged view of Fig. 6 is shown in Fig. 7. Apart from the convergence time, the rise time of fractional order method is smaller as compared to integer order method. From [20], [21], it is clear that algebraic method is robust to noise and nonzero initial conditions. To simulate the effects of noise, band limited white noise is added to the loading torque signal T_L. The composite signal is given as input to algebraic parameters estimation algorithm. The noisy signal is shown in Fig. 8. The parameters of noise signal are selected as follows: noise power ($n_p = 0.0001$), noise samples ($n_s = 0, 001$) and initial seeds 100. The estimated parameters with noise are shown in Fig. 9. From the simulation results, it is clear that the integer order algebraic method is robust against noise, but at the same time, the estimated parameters oscillate about the nominal values. However in case of non-integer method, the oscillations reduce significantly and the estimated parameters remain in the vicinity of the nominal parameters. So the proposed method is more appropriate from the implementation point of view.

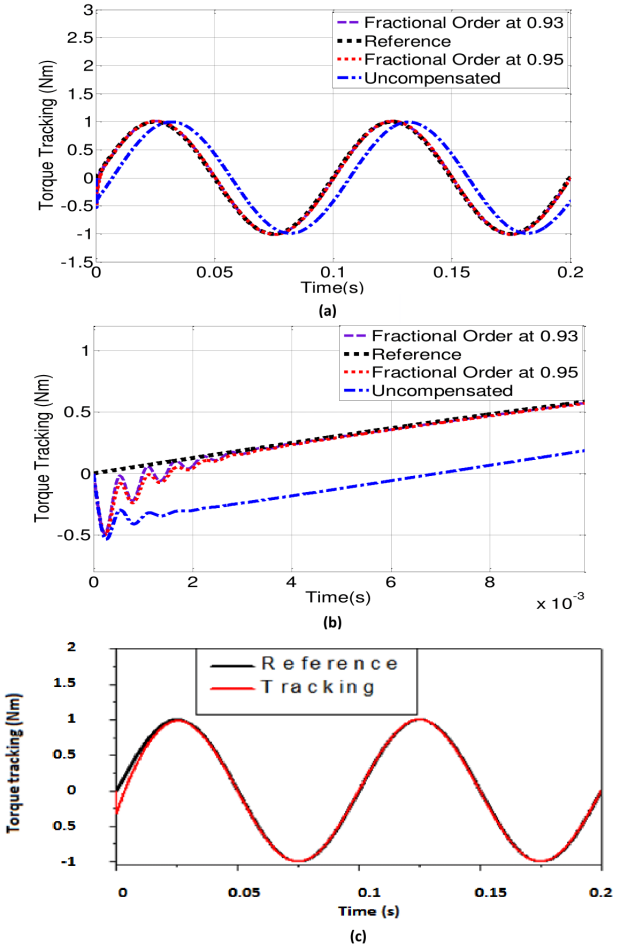

FIGURE 13. (a) Torque tracking using fractional order controller (b) Enlarged view(c) Torque tracking using integer order controller.

C. EXTRA TORQUE AND FRICTION ESTIMATION

The reference command of ELS loading motor is: $T_r = 2\pi ft$ with frequency of 10 Hz. Extra torque disturbance is estimated using Eq. (41). Fig. 10a and 10b show estimated extra torque using integer and non-integer methods. From Fig. 10a, the extra torque using integer order adaptive fuzzy system is accurately estimated. It is already confirmed from Fig. 5a that in case of integer order dynamics extra torque disturbance is less in magnitude. From Fig. 10b, the magnitude of estimated extra torque with $\alpha = 0.95$ and $\alpha = 0.93$ is large as compared to the integer order. Since dynamics of fractional order ELS system is faster. So in-spite of large estimated extra torque, fractional order adaptive fuzzy system is superior to the integer order version as it will ensure improved transient performance. Fig. 11a shows the phase response of the estimated extra torque. Phase of the estimated extra torque with $\alpha = 0.93$ is leading which in turn improves transient response of the proposed control. Friction torque compensation is shown in Fig. 11b. To avoid noisy feedback, estimated state vector $[\hat{T}_L\ \dot{\hat{T}}_L]$ is used. The estimation results are compared in Fig. 12a and 12b. From the author's previous work [1], with the same gain matrix $[\Gamma_1, \Gamma_2]$, fractional order state estimator

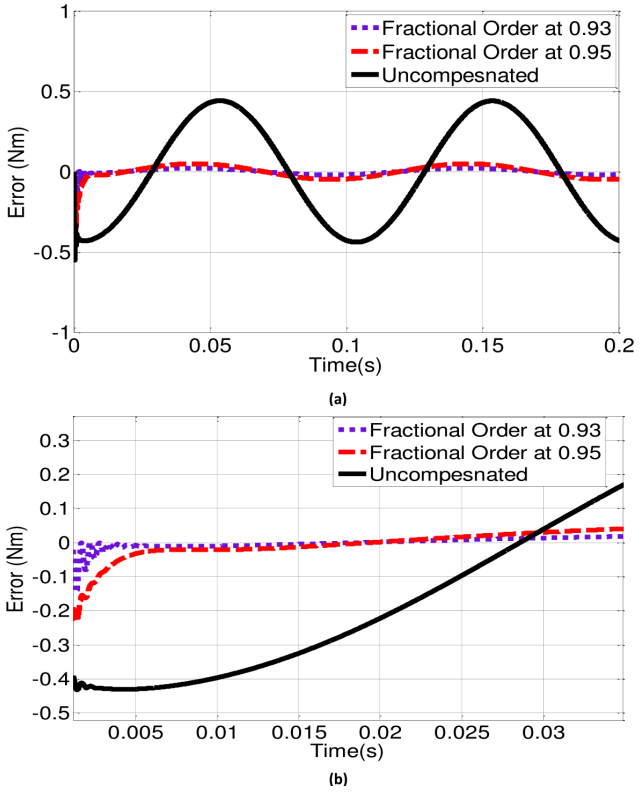

FIGURE 14. (a) Torque tracking Error (b) Enlarged view.

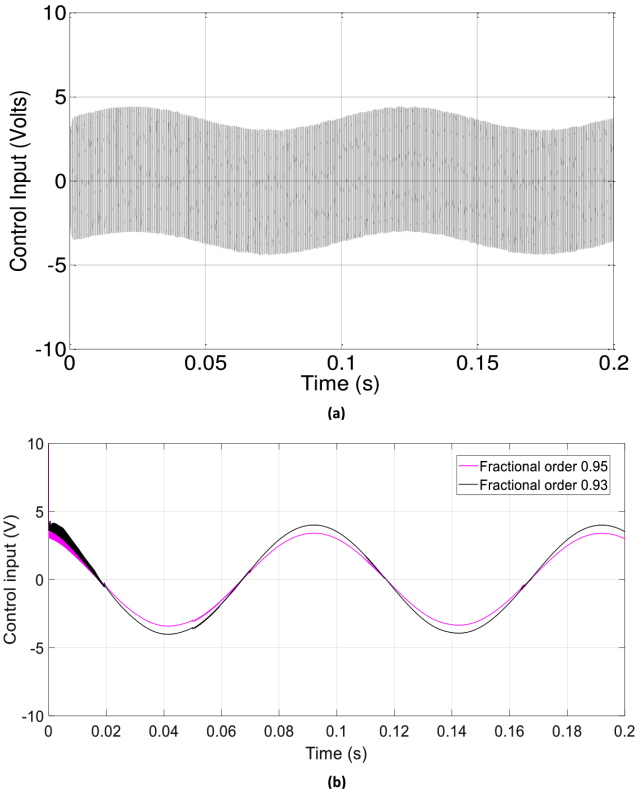

FIGURE 15. Control input (a) Integer order controller (b) Proposed controller.

ensures noise free state estimation. Here $[\Gamma_1, \Gamma_2]$ represent the gains of the state estimator.

D. TORQUE TRACKING SIMULATION

The reference command of ELS torque motor is $T_r = 2\pi ft$ with frequency 10 Hz. Fig. 13a shows the torque tracking performance using ideal measured states. Enlarged view of Fig. 13a is shown in Fig. 13b. Torque tracking response using integer order controller is shown in Fig. 13c. From the comparison it is concluded that the initial transient response of the proposed controller is faster as compared to the integer order controller. As compared to author's previous work "Fig. 8a" [1], the transient performance under the proposed control scheme significantly improves. From [1], excellent transient performance were achieved using transient performance controller while in this work the proposed controller is much simpler. Tracking error comparisons are given in Fig. 14a and 14b. From the results presented it is concluded that the proposed control law with $\alpha = 0.93$ ensures minimum tracking error. Under the proposed method, the control signal exhibits reduced chattering phenomena. This fact is conformed from the simulation results presented in Fig. 15a and 15b. From Eq. (36), If the fractional order is set as: $\alpha = 1$, then the remaining expression of the equation represents the integer order version of proposed controller. Fig. 15a shows the control signal simulations using integer order method. The control signal contains high frequency chattering and thus it is not feasible for practical implementation. Fig. 15b shows the control signal simulations using non-integer method. By utilizing the proposed control method, chattering phenomena significantly reduces. This is due to the fractional order integration of the discontinuous function represented as $-\frac{1}{b_u} D^{\alpha-1}[k_1 e_2 + k_2 . sgn(e_2)]$.

E. TIME VARYING PARAMETERS SIMULATIONS

To simulate the effect of time varying parameters, the un-modeled disturbance $d_{p(t)} = \Delta a(t)\dot{T}_L + \Delta b(t)u_q$ is assumed to be a sinusoidal type function varying with time. Fig. 16 compares the $\frac{\hat{\Psi}(t)}{b}$ adaptation using integer order control [1] and the proposed method. Un-modeled disturbance is applied at $t = 0.08$ sec. In comparison to the integer order method, adaptation of $\frac{\hat{\Psi}(t)}{b}$ using the proposed method is faster. Although the control effort using the proposed method is a little more but it is still within the saturation limit of the drive stage. Fig. 17 shows $\frac{\hat{\Psi}(t)}{b}$ adaptation when the system is subject to un-modeled disturbance and measurement noise. With noisy states $\frac{\hat{\Psi}(t)}{b}$ adaptation using the proposed algorithm with $\alpha = 0.93$ is less corrupted by the measurement noise as compared to the integer order algorithm [1]. So the proposed algorithm is feasible from the practical implementation point of view. Enlarged view of Fig. 17 is shown in Fig. 18. From the simulation results presented in Fig. 18,

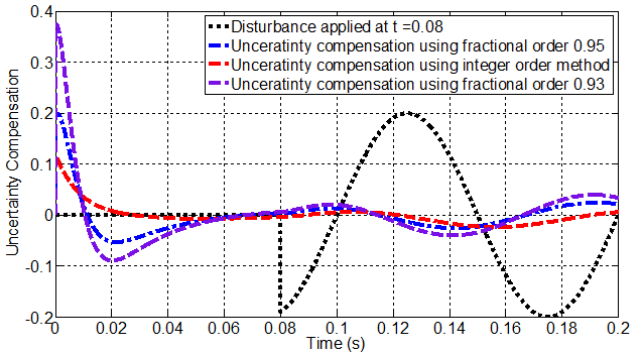

FIGURE 16. $\frac{\hat{\Psi}(t)}{b}$ **Adaptations with Time Varying Parameters.**

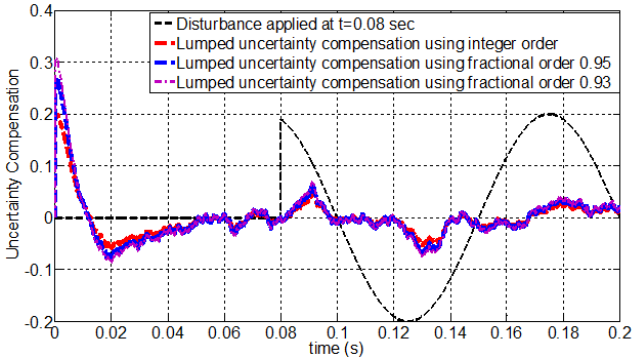

FIGURE 17. $\frac{\hat{\Psi}(t)}{b}$ **adaptations with time varying parameters and noise.**

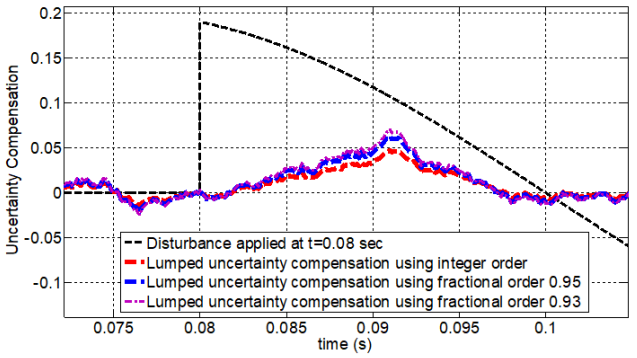

FIGURE 18. **Enlarged view for** $\frac{\hat{\Psi}(t)}{b}$ **adaptations with time varying parameters and noise.**

the response of fractional order method with $\alpha = 0.93$ is faster and $\frac{\hat{\Psi}(t)}{b}$ adaptation is smooth.

V. CONCLUSION

In this article a fractional order adaptive fuzzy back-stepping torque control is proposed for ELS system using fractional order dynamics. The proposed method eliminates the use of transient performance controller [1] and ensures good transient performance. Similarly high frequency chattering is significantly reduced. Fractional order algebraic method offers more degrees of freedom to adjust the convergence speed and overshoots in the estimated parameters with noisy measurements. Moreover adaptation response of fractional order adaptive laws is faster as compared to integer order methods. The faster the adaptation, the more robust is the controller. Fractional order adaptation is also less corrupted from measurement noise.

APPENDIX A

$$A_{11} = -\int^{\alpha} t^3 T_L + 9\int^{\alpha+1} t^2 T_L - 18\int^{\alpha+2} tT_L + 6\int^{\alpha+3} T_L$$

$$A_{21} = -\int^{\alpha+1} t^3 T_L + 9\int^{\alpha+2} t^2 T_L - 18\int^{\alpha+3} tT_L + 6\int^{\alpha+4} T_L$$

$$A_{31} = -\int^{\alpha+2} t^3 T_L + 9\int^{\alpha+3} t^2 T_L - 18\int^{\alpha+4} tT_L + 6\int^{\alpha+5} T_L$$

$$A_{12} = \int^{\alpha+1} t^3 u - 6\int^{\alpha+2} t^2 u + 6\int^{\alpha+3} tu$$

$$A_{22} = \int^{\alpha+2} t^3 u - 6\int^{\alpha+3} t^2 u + 6\int^{\alpha+4} tu$$

$$A_{32} = \int^{\alpha+3} t^3 u - 6\int^{\alpha+4} t^2 u + 6\int^{\alpha+5} tu$$

$$A_{13} = -\int^{\alpha+1} t^3 T_L + 6\int^{\alpha+2} t^2 T_L - 6\int^{\alpha+3} tT_L$$

$$A_{23} = -\int^{\alpha+2} t^3 T_L + 6\int^{\alpha+3} t^2 T_L - 6\int^{\alpha+4} tT_L$$

$$A_{33} = -\int^{\alpha+3} t^3 T_L + 6\int^{\alpha+4} t^2 T_L - 6\int^{\alpha+5} tT_L$$

$$B_1 = t^3 T_L - 3(3+\alpha)\int t^2 T_L + 3(3+\alpha)(2+\alpha)\int^{2} tT_L - (3+\alpha)(2+\alpha)(1+\alpha)\int^{3} T_L$$

$$B_2 = \int t^3 T_L - 3(3+\alpha)\int^{2} t^2 T_L + 3(3+\alpha)(2+\alpha)\int^{3} tT_L - (3+\alpha)(2+\alpha)(1+\alpha)\int^{4} T_L$$

$$B_3 = \int^{2} t^3 T_L - 3(3+\alpha)\int^{3} t^2 T_L + 3(3+\alpha)(2+\alpha)\int^{4} tT_L - (3+\alpha)(2+\alpha)(1+\alpha)\int^{5} T_L$$

APPENDIX B

[a b c]	system parameters
$[a_n b_n c_n]$	nominal parameters
$[\Delta a(t)\ \ \Delta b(t)]$	slow time varying parameters
$[\Omega_1\ \Omega_2\ \Omega_3\ \Omega_4]$	domain of parameters uncertainty
$[a_{\min}\ b_{\min}\ c_{\min}]$, $[a_{\max}\ b_{\max}\ c_{\max}]$	bounds of parameters
$d_{p(t)}$	disturbance term due to slow time varying parameters
d_{ef}	fuzzy approximation error
$\Psi(t)$	Lumped disturbance due to fuzzy approximation error and slow time varying disturbance

$\hat{\Psi}(t)$	Estimated $\Psi(t)$
$[u_d\ u_q]$	voltage in d and q axis
$[i_d\ i_q]$	current in d and q axis
$[i_d * \ i_q*]$	Extra induced current in d and q axis due to actuator,s movement
i_{dr}	d axis reference current
$\theta*$	Unknown Parameter vector
R_s	stator winding resistance
$[L_{sq}\ L_{sd}]$	Stator winding inductance in dq frame
$[w_m\ w_a]$	Loading motor and actuator angular speed
$[\theta_m\ \theta_a]$	Loading motor and actuator angular position
$[P\ \ \Psi_m]$	Number of pole pairs and magnetic flux of rotor
$[J\ \ B]$	Total inertia and damping coefficient
$[T_e\ T_f\ T_L]$	Electromagnetic, friction and loading torque
T_e*	Induced electromagnetic torque in loading motor due to actuator movement
T_{sft}	Mechanical torque due to actuator movement when input command of loading motor is zero $[K_t\ K_b\ K_s]$ Motor torque constant, back emf constant and total stiffness of torque sensor and shaft
$f(T_{extra}, T_f)$	Nonlinear function representing extra torque and friction torque
$\hat{f}(T_{extra}, T_f)$	Estimated nonlinear function representing extra torque and friction torque
α_1, V_1, V_2	First virtual control, first and second Lyapunov functions
$\gamma\ , \gamma_1,\ \gamma_2,\ \eta_i$	Learning rates for adaptive laws
$[u_r\ \hat{u}_r]$	Fixed gain and transient performance controller
$f(d_{p(t)}, d_{ef})$	Nonlinear function representing slow time varying and fuzzy estimation error
$[\hat{T}_L\ \hat{\dot{T}}_L]$	Estimated state vector
$[(e_1\ \dot{e}_1), e\ ]$	Error vector, error between ELS system and state predictor
$[k_1\ , k_2\ , q_1, q_2]$	Controller parameters
$[T_r\ \dot{T}_r]$	Reference torque command vector
$\Gamma_{1,2}$	State predictor gain
E	Error vector between ELS plant and state predictor

REFERENCES

[1] J.-C. Mare, "Dynamic loading systems for ground testing of high speed aerospace actuators," *Aircr. Eng. Aerosp. Technol.*, vol. 78, no. 4, pp. 275–282, 2006, doi: 10.1108/17488840610675546.

[2] N. Ullah and S. Wang, "Torque controller design for electrical load simulator with estimation and compensation of parametric uncertainty," in *Proc. 9th Int. Bhurban Conf. Appl. Sci. Technol. (IBCAST)*, 2012, pp. 15–21.

[3] Z. Jiao, C. Li, and Z. Ren, "Extraneous torque and compensation control on the electric load simulator," in *Proc. 5th Int. Symp. Instrum. Control Technol.*, 2003, pp. 723–727.

[4] J. Yao, Z. Jiao, and D. Ma, "A practical nonlinear adaptive control of hydraulic servomechanisms with periodic-like disturbances," *IEEE/ASME Trans. Mechatronics*, vol. 20, no. 6, pp. 2752–2760, Dec. 2015.

[5] J. Yao, W. Deng, and Z. Jiao, "Adaptive control of hydraulic actuators with LuGre model-based friction compensation," *IEEE Trans. Ind. Electron.*, vol. 62, no. 10, pp. 6469–6477, Oct. 2015.

[6] X. Wang, S. Wang, and X. Wang, "Electrical load simulator based on velocity-loop compensation and improved fuzzy-PID," in *Proc. IEEE Int. Symp. Ind. Electron.*, Jul. 2009, pp. 238–243.

[7] X. Wang, S. Wang, and B. Yao, "Adaptive robust torque control of electric load simulator with strong position coupling disturbance," *Int. J. Control, Automat. Syst.*, vol. 11, pp. 325–332, Apr. 2013.

[8] L. Yunhua, "Development of hybrid control of electrohydraulic torque load simulator," *J. Dyn. Syst., Meas. Control*, vol. 124, pp. 415–419, Sep. 2002.

[9] J. Yao, Z. Jiao, and D. Ma, "High dynamic adaptive robust control of load emulator with output feedback signal," *J. Franklin Inst.*, vol. 351, no. 8, pp. 4415–4433, 2014.

[10] J. Yao, Z. Jiao, and B. Yao, "Nonlinear adaptive robust backstepping force control of hydraulic load simulator: Theory and experiments," *J. Mech. Sci. Technol.*, vol. 28, no. 4, pp. 1499–1507, 2014.

[11] J. Yao, Z. Jiao, and D. Ma, "Extended-state-observer-based output feedback nonlinear robust control of hydraulic systems with backstepping," *IEEE Trans. Ind. Electron.*, vol. 61, no. 11, pp. 6285–6293, Nov. 2014.

[12] J. Yao, Z. Jiao, D. Ma, and L. Yan, "High-accuracy tracking control of hydraulic rotary actuators with modeling uncertainties," *IEEE/ASME Trans. Mechatronics*, vol. 19, no. 2, pp. 633–641, Apr. 2014.

[13] N. Ullah and S. Wang, "State observer based adaptive fuzzy backstepping compensation control of passive torque simulator," *Przegląd Elektrotechniczny*, vol. 89, no. 2a, pp. 160–165, 2013.

[14] J. Yao, Z. Jiao, and B. Yao, "Robust control for static loading of electrohydraulic load simulator with friction compensation," *Chin. J. Aeronaut.*, vol. 25, pp. 954–962, Dec. 2012.

[15] J. Yao, Z. Jiao, and S. Han, "Friction compensation for low velocity control of hydraulic flight motion simulator: A simple adaptive robust approach," *Chin. J. Aeronaut.*, vol. 26, pp. 814–822, 2013.

[16] J. Yao, Z. Jiao, B. Yao, Y. Shang, and W. Dong, "Nonlinear adaptive robust force control of hydraulic load simulator," *Chin. J. Aeronaut.*, vol. 25, no. 5, pp. 766–775, 2012.

[17] B. S. Kim and S. I. Han, "Non-linear friction compensation using backstepping control and robust friction state observer with recurrent fuzzy neural networks," *Proc. Inst. Mech. Eng., I, J. Syst. Control Eng.*, vol. 223, pp. 973–998, Jun. 2009.

[18] B. K. Yoo and W. C. Ham, "Adaptive control of robot manipulator using fuzzy compensator," *IEEE Trans. Fuzzy Syst.*, vol. 8, no. 2, pp. 186–199, Apr. 2000.

[19] Y. Pan, M. J. Er, D. Huang, and Q. Wang, "Adaptive fuzzy control with guaranteed convergence of optimal approximation error," *IEEE Trans. Fuzzy Syst.*, vol. 19, no. 5, pp. 807–818, Oct. 2011.

[20] J. Becedas, G. Mamani, and V. Feliu, "Algebraic parameters identification of DC motors: Methodology and analysis," *Int. J. Syst. Sci.*, vol. 41, no. 10, pp. 1241–1255, 2012.

[21] A. Luviano-Juárez, J. Cortés-Romero, and H. Sira-Ramírez, "Algebraic identification and control of an uncertain DC motor using the delta operator approach," in *Proc. 7th Int. Conf. Elect. Eng. Comput. Sci. Autom. Control*, 2012, pp. 482–487.

[22] L. Shuxi, W. Mingyu, and L. Taifu, "Research on direct torque control based asynchronous dynamometer for dynamic emulation of mechanical loads," *Kybernetes*, vol. 39, pp. 1018–1028, Jun. 2010.

[23] G. Zhang, H. Chen, and C. Zhou, "A novel estimate method for the speed and mechanical torque of the AC asynchronous electrical dynamometer," *Int. J. Circuit Syst. Signal Process.*, vol. 1, no. 3, pp. 232–238, 2010.

[24] G. C. D. Sousa and D. R. Errera, "A high performance dynamometer for drive systems testing," in *Proc. 23rd Int. Conf. Ind. Electron., Control, Instrum.*, vol. 2, 1997, pp. 500–504.

[25] J. Chauvin and A. Chasse, "Dynamic periodic observer for a combustion engine test bench," in *Proc. 48th IEEE Conf. Decis. Control (CDC) Held Jointly 28th Chin. Control Conf.*, Dec. 2009, pp. 6608–6613.

[26] P. Ortner, E. Gruenbacher, and L. del Re, "Model based nonlinear observers for torque estimation on a combustion engine test bench," in *Proc. IEEE Int. Conf. Control Appl.*, Sep. 2008, pp. 221–226.

[27] A. Oustaloup, X. Moreau, and M. Nouillant, "The CRONE suspension," *Control Eng. Pract.*, vol. 4, no. 8, pp. 1101–1108, Aug. 1996.

[28] N. Ullah, W. Shaoping, M. I. Khattak, and M. Shafi, "Fractional order adaptive fuzzy sliding mode controller for a position servo system subjected to aerodynamic loading and nonlinearities," *Aerosp. Sci. Technol.*, vol. 43, pp. 381–387, Jun. 2015.
[29] M. P. Aghababa, "A Lyapunov-based control scheme for robust stabilization of fractional chaotic systems," *Nonlinear Dyn.*, vol. 78, no. 3, pp. 2129–2140, 2014.
[30] Y. Wei, D. Sheng, Y. Chen, and Y. Wang, "Fractional order chattering-free robust adaptive backstepping control technique," *Nonlinear Dyn.*, vol. 95, no. 3, pp. 2383–2394, 2019.
[31] N. Ullah, A. Ullah, A. Ibeas, and J. Herrera, "Improving the hardware complexity by exploiting the reduced dynamics-based fractional order systems," *IEEE Access*, vol. 5, pp. 7714–7723, 2017, doi: 10.1109/ACCESS.2017.2700439.
[32] W. Yu, Y. Luo, and Y. Pi, "Fractional order modeling and control for permanent magnet synchronous motor velocity servo system," *Mechatronics*, vol. 23, no. 7, pp. 813–820, 2013, doi: 10.1016/j.mechatronics.2013.03.012.
[33] A. Mujumdar, B. Tamhane, and S. Kurode, "Fractional order modeling and control of a flexible manipulator using sliding modes," in *Proc. Amer. Control Conf.*, Portland, OR, USA, Jun. 2014, pp. 2011–2016, doi: 10.1109/ACC.2014.6858955.
[34] M. S. Sarafraz and M. S. Tavazoei, "Passive realization of fractional-order impedances by a fractional element and RLC components: Conditions and procedure," *IEEE Trans. Circuits Syst. I, Reg. Papers*, vol. 64, no. 3, pp. 585–595, Mar. 2017, doi: 10.1109/TCSI.2016.2614249.
[35] S. S. Ray, S. Sahoo, and S. Das, "Formulation and solutions of fractional continuously variable order mass–spring–damper systems controlled by viscoelastic and viscous–viscoelastic dampers," *Adv. Mech. Eng.*, vol. 8, no. 5, pp. 1–13, 2016, doi: 10.1177/1687814016646505.
[36] R. Cipin, C. Ondrusek, and R. Huzlík, "Fractional-order model of DC motor," in *Mechatronics*, T. Březina and R. Jabloński, Eds. Cham, Switzerland: Springer, 2013.
[37] Y. Wei, P. W. Tse, Z. Yao, and Y. Wang, "Adaptive backstepping output feedback control for a class of nonlinear fractional order systems," *Nonlinear Dyn.*, vol. 86, no. 2, pp. 1047–1056, 2016.
[38] D. Xue, Y. Q. Chen, and D. P. Atherton, *Linear Feedback Control: Analysis and Design With MATLAB*, 1st ed. Philadelphia, PA, USA: Society for Industrial and Applied Mathematics, 2009. [Online]. Available: https://www.amazon.com/Linear-Feedback-Control-Analysis-Advances/dp/0898716381
[39] N. Ullah, W. Khan, and S. Wang, "High performance direct torque control of electrical aerodynamics load simulator using fractional calculus," *Acta Polytechnica Hungarica*, vol. 11, no. 10, pp. 59–78, 2014.
[40] Y. Wei, Y. Chen, S. Liang, and Y. Wang, "A novel algorithm on adaptive backstepping control of fractional order systems," *Neurocomputing*, vol. 165, pp. 395–402, Oct. 2015.
[41] D. Matignon, "Stability properties for generalized fractional differential systems," in *Proc. ESAIM*, vol. 5, 1998, pp. 145–158.
[42] I. Podlubny, "The Laplace transform method for linear differential equations of the fractional order," in *Institute of Experimental Physics*. Bratislava, U.K.: Slovak Academy of Sciences, 1994, pp. 1–29.

NASIM ULLAH received the Ph.D. degree in mechatronic engineering from Beihang University, Beijing, China, in 2013. From September 2006 to 2010, he was a Senior Design Engineer with IICS, Pakistan. He is currently an Associate Professor of electrical engineering with Taif University, Saudi Arabia. His current research interests include renewable energy, flight control systems, the integer and fractional order modeling of dynamic systems, integer/fractional order adaptive robust control methods, fuzzy/NN, hydraulic and electrical servos, epidemic, and vaccination control strategies.

AHMAD AZIZ AL-AHMADI received the Ph.D. degree in nano-electronic devices from the School of Engineering, Ohio University, Athens, OH, USA. He is currently an Associate Professor with the Department of Electrical Engineering, Faculty of Engineering, Taif University, Saudi Arabia, where he has been the Vice-Dean of the Faculty of Engineering, since July 2017. His current research interest includes nano-electronic devices.